Photoelastic stress analysis of mode I fracture toughness tests using PMMA samples

IOP Conf. Series: Earth and Environmental Science **833** (2021) 012031 doi:10.1088/1755-1315/833/1/012031

Photoelastic stress analysis of mode I fracture toughness tests using PMMA samples

A Muñoz-Ibáñez, M Herbón-Penabad, J Delgado-Martín

School of Civil Engineering, Universidade da Coruña, Campus de Elviña s/n, A Coruña, 15071, Spain

andrea.munoz@udc.es

Abstract. Rocks are usually inhomogeneous and anisotropic materials. The presence of foliation planes, grain boundaries or even microcracks may alter the stress distribution. In order to identify whether unusual behaviours in rocks are due to these imperfections or result from other factors (e.g. experimental configuration), the analyses of homogenous and isotropic materials is an useful approach. We have performed a series of mode I fracture toughness (K_{IC}) tests using polymethyl methacrylate (PMMA) samples, which has the advantage of allowing photoelastic stress analysis based on its birefringent nature. Three different testing configurations were considered in the study: S\ emi-circular bend (SCB) test, the *pseudo*-compact tension (*p*CT) test, and a new alternative configuration based on the previous two that we have called *pseudo*-SCB (*p*SCB) test. To perform the photoelastic analysis, all the experiments were complemented with a specially-designed experimental setup consisting in two orthogonally arranged circular polarizers placed on both sides of the tested specimens. Using a source of white (polychromatic) light on one end it is possible to record the stress distribution using a digital camera aligned with the samples on the other end. As the load increases, a distinct evolving pattern of colour fringes can be visualized in the samples illustrating the spatially distributed stress levels. Based on this analysis we observe in some of the tests performed non-symmetrical stress fields. Although this behaviour could be related with the testing configuration, results suggest that other features, such as the shape of the notch tip, imperfections in sample preparation, or the misalignment of the samples in the testing device may also have an influence in stress distribution.

1. Introduction

Rock materials are usually discontinuous at all scales [1]. At the microscale, the presence of pores, grain boundaries, and pre-existing fractures can lead to high stress concentrations under increasing load. At the macroscale, foliation or bedding planes are characterized by having lower resistance and represent zones of weakness. These discontinuities might be determinant in fracture growth and, therefore, play an important role in the success of engineering projects involving rock materials (e.g., hydraulic fracturing, nuclear waste disposal or geothermal energy). Mode I fracture toughness (K_{IC}) represents the resistance of a material to the propagation of tensile cracks under the presence of pre-existing discontinuities. In K_{IC} assessment in rocks, properties such as grain size, particle arrangement, or the degree of cementation can determine the propagation path of the cracks [2]. To identify additional factors the use transparent models made of materials such as polymers, resins or glass is an interesting approach specially to visualize fracture development. For instance, Wu et al [3] monitored the process

of crack growth on hydraulic fracture tests using polymeric samples. Their results suggest that far-field stresses determine the orientation of the final fracture orientation but have little effect on fracture initiation. Although the materials used in this type of studies are usually homogeneous and have, therefore, a limited ability to improve the understanding about the behavior of heterogeneous samples, they are valuable to identify additional factors (e.g. geometrical features, loading conditions) that can have an effect on fracture propagation.

Photoelasticity is a non-destructive testing technique used to visualize stress distributions and determine points of stress concentration in a material subjected to an external load. The method is based on the opto-mechanical coupling of birefringent materials, which is characteristic of many common transparent polymers [4]. A birefringent material, when properly aligned with other elements (i.e., light source, polarizers, retarders), will exhibit chromatic fringe patterns as a function of the applied stress. If polarized white (polychromatic) light travels across a birefringent stressed material, some characteristic optical features develop: dark bands (or isoclines) and colored fringes (or isochromes). The isochromes represent lines of constant principal stress difference in a plane normal to the direction of light propagation, while the isoclines indicate locations with the same direction of the principal stresses [5]. In rock mechanics, photoelastic birefringent materials can be used to investigate stress patterns arising from specific testing methods and for model matching.

In this study we have carried out K_{IC} tests using polymethyl methacrylate (PMMA) samples. This material was selected not only for being homogeneous and isotropic but also for its birefringent properties, which allow performing photoelastic stress analysis (PSA) concurrent to test execution. The study has been focused in three different testing methodologies: i) the semi-circular bend (SCB) test, which is one of the suggested methods proposed by the International Society for Rock Mechanics [6]; ii) the pseudo-compact tension (*p*CT) test, recently proposed by to assess K_{IC} in rocks under pure tensile conditions [2]; and iii) the pseudo-semi-circular bend (*p*SCB) test, which can be regarded as a combination of the two mentioned testing methods, and that is further described in [7]. In this work, the K_{IC} values of PMMA derived with the three methodologies are discussed, while the stress distribution in the samples was also investigated.

2. Materials and methods

2.1. Materials and sample preparation

PMMA, also known with the trade-names of Perspex®, Plexiglass®, or Lucite®, is a transparent brittle-elastic polymer of high strength and rigidity [3,9]. Reference values for the compressive strength (83-124 MPa), tensile strength (30-76 MPa) or elastic modulus (2950-3300 MPa) of this material at room temperature are reported in the literature [9,10].

Table 1. PMMA specimen dimensions: D = diameter; B = thickness; a/b or a/R = notch length ratio; R = radius; s/D = span length; G_d = U-shaped groove depth; G_w = U-shaped groove width.

Method	D (mm)	B (mm)	a/R or a/b	s/D	G_w (mm)	G_d (mm)
SCB	50	25	0.28-0.60	0.8	-	-
*p*CT	50	25	0.50-0.75	-	10	5
*p*SCB	50	25	0.50-0.75	-	10	5

In this study, samples for fracture toughness tests were obtained from 50-mm diameter PPMA bars, which were sliced into discs (thickness-to-diameter ratio of ~0.5) using a lathe. For the SCB specimens, the discs were halved and a straight notch was cut in the center of the flat surface. In the *p*CT and *p*SCB specimens, a U-shape groove was carved in the discs to allow sample loading, and a straight notch was also cut to act as stress concentrator. Subsequently, the surfaces of the samples perpendicular to the ray of light were polished to enhance fringe visualization. We considered a range of notch length ratios for

each testing method. Dimensions of the samples are given in table 1 and a schematic illustration of the three geometries is shown in figure 1. It should be noted that the PMMA specimens were not annealed after machining. Consequently, we would expect observing a residual stress field in the samples before testing.

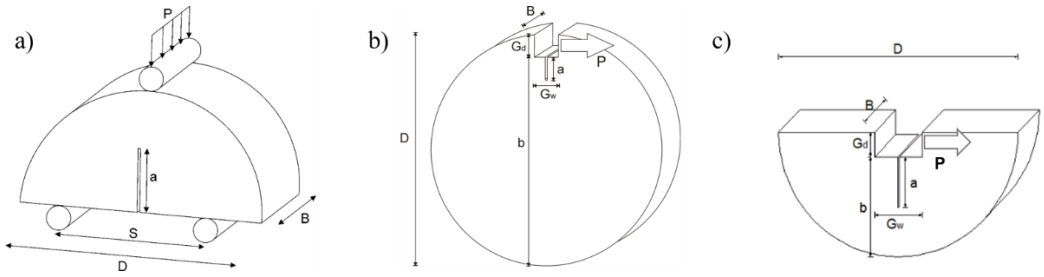

Figure 1. Specimen geometries and loading configuration. a) SCB test; b) *p*CT test; c) *p*SCB test.

2.2. Fracture toughness testing setups

Mode I fracture toughness tests were performed following three different experimental approaches: SCB, *p*CT, and *p*SCB methods. The corresponding setups are illustrated in figure 2. SCB specimens were tested following the recommendations of the ISRM [6] with a three-point bending fixture located in a servo-electric frame equipped with a 4,5 kN load cell. In this configuration the sample is supported by two steel rollers (separated a fixed distance, *s*). A third roller is used to deliver the load to the top of the sample. In this work, the span length (*s/D*) was set to 0.8 as suggested for testing strong materials. *p*CT and *p*SCB experiments were carried out following the procedure described in [2]. Tests were performed with a specially-designed testing device equipped with a 50 kN load cell. All the experiments were conducted at room conditions with a constant displacement rate of 0.1 mm/min. Load (*P*) and load point displacement (LPD) were recorded continuously during testing. LPD corresponds to the displacement of the loading roller in the SCB tests, and to the movement of the steel jaw in *p*CT and *p*SCB tests.

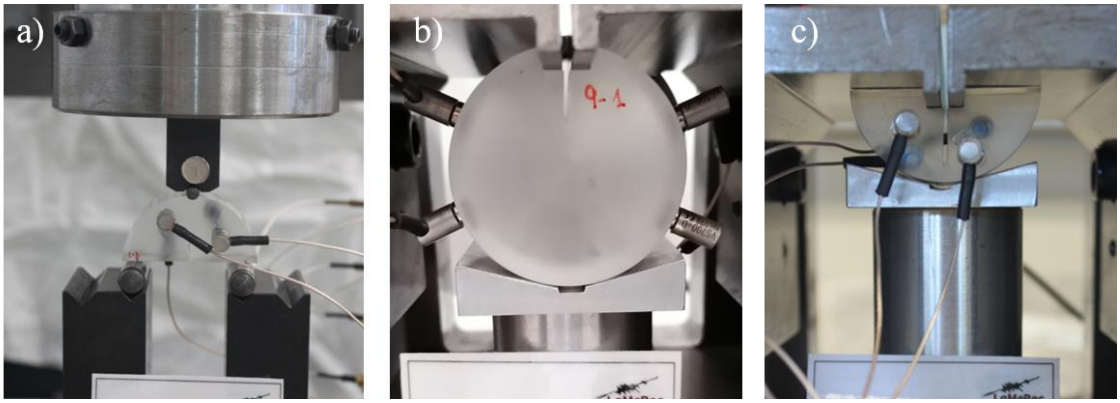

Figure 2. Experimental setup for mode I fracture toughness tests. a) SCB; b) *p*CT; c) *p*SCB.

Level I testing was considered in this study and, therefore, only the value of maximum load (P_{max}) recorded was considered to compute mode I fracture toughness. K_{IC} was calculated using the expressions given in [6] for the SCB specimens, and in [2] for the *p*CT and *p*SCB specimens. For the latter method, the expression of the dimensionless stress intensity factor (Y') derived for 50 mm- diameter specimens is given in [7].

2.3. Photoelastic setup

A polariscope was used for visualizing the stress field on the tested specimens (figure 3). The setup consists of a source of led white light and two 82 mm-diameter circular polarizers (K&F Concept) equipped with ¼-λ waveplates (or retarders). The configuration of the setup is cross-polar (i.e. the polarizer, next to the light source, and the analyser, next to the camera, polarize light at 90º) with the sample located between the two filters. With no sample, the cross-polar configuration produces light beam extinction (i.e. a dark field) while the insertion of the sample illuminates the field with coloured (isochromes) and black (isoclines) fringes whose development is related with the stress distribution in the sample: A non-stressed sample will theoretically result in a single isochrome occupying the whole surface of the sample. The experiments were recorded with a digital camera (KOPACE, KP-2100) with a resolution of 1920x1080 pixels and a frame rate of 60 f/s.

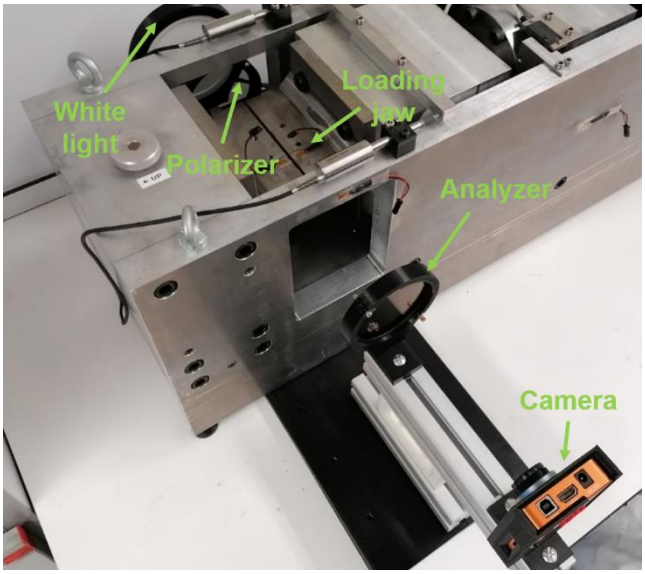

Figure 3. PSA setup attached to the testing equipment used to perform *p*CT tests.

3. Results and discussion

3.1. Mode I fracture toughness assessment

Typical load-displacement (*P*-LPD) curves obtained from the experiments are plotted in figure 4. We observe that load increases linearly (elastic phase) up to P_{max}. Afterwards the sample fails abruptly, proving the brittleness of the material and in agreement with the behaviour reported by Torabi et al [10] for PMMA samples loaded under mixed mode I/III. As previously discussed in [2] for rock samples, the *p*CT test configuration allows good control on fracture propagation even in the post-peak behaviour: the material losses strength but still retains some cohesion. This is also evidenced by the loading curves recorded for the *p*SCB sample geometry. Contrary, because the SCB configuration is more prone to elastic energy storage, its release at the critical stress leads to a fast, uncontrolled fracture propagation.

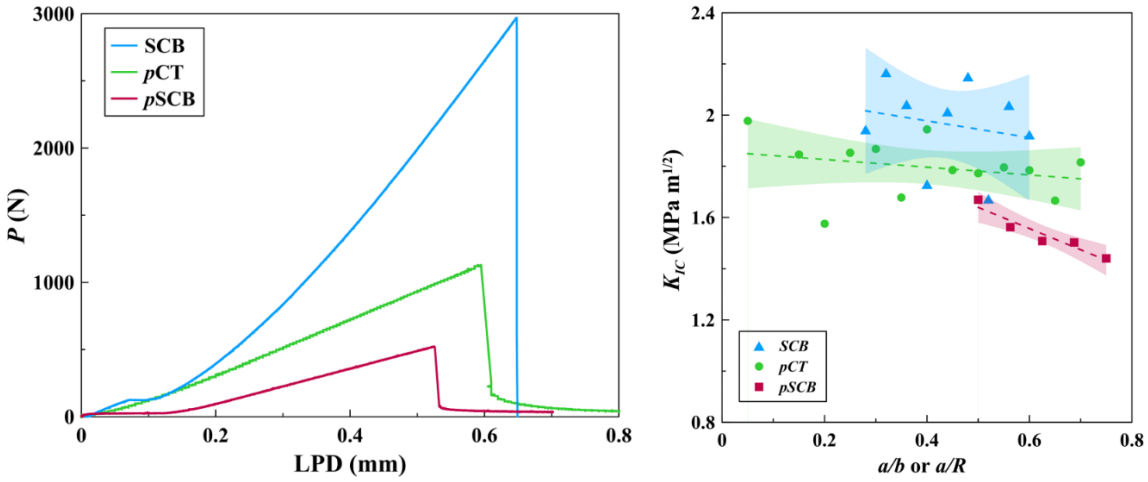

Figure 4. Load vs load point displacement (*P*-LPD) curves (left); and mode I fracture toughness (K_{IC}) vs notch length ratio (right).

Mode I fracture toughness results obtained from the SCB, *p*CT, and *p*SCB tests have been plotted as a function of notch length ratio in figure 4. SCB tests result in the higher K_{IC} values while the lower ones correspond to the *p*SCB tests. Apparently, fracture toughness has some dependence on the ligament length for the ranges considered in this study, with decreasing values for larger notches (i.e., shorter ligaments). This behaviour has been also observed by Visser et al [11] in PMMA samples during tensile impact testing. In our experiments, this effect appears to be more prominent in the case of the *p*SCB specimens.

Although a graphical analysis can be useful as a first approach, we opted for performing statistical analysis with the aid of the free software Past 3.0 [12] to get quantitative information about test repeatability and reproducibility. To this aim, first we split the values of K_{IC} obtained from the experiments into three groups according to the testing method. Then, we performed two statistical checks considering a significance level of 95%: i) a within-group analysis of repeatability aimed at assessing normality through a non-parametric Shapiro-Wilk test, and ii) a between-group analysis focused on the comparison of means and based on a one-way analysis of variance (ANOVA) and the non-parametric Mann-Whitney pairwise test. The three groups considered conform to normal distributions, which suggests that the length of the notch might not be a determinant factor on the assessment of K_{IC}. Contrary, the between-group analysis to assess reproducibility was unsuccessful in the three cases considered. This may be indicating a strong dependence of fracture toughness on the testing conditions and sample geometry for this kind of material, in agreement with what we can perceive from the plots. Mean values of K_{IC} are given in table 2 for each testing method. We observe that K_{IC} has the lowest variability in the case of the *p*CT test, even considering a broader range of notch length ratios than for the SCB and *p*SCB tests. This behaviour agrees with that observed previously by Muñoz-Ibáñez et al [13] for *p*CT and SCB tests performed with four different rock types.

Table 2. Mode I fracture toughness (K_{IC}) values (mean ± standard error of the mean) for PMMA samples. Number of experiments is given into brackets.

Method	K_{IC} (MPa m$^{1/2}$)
SCB	1.96 ± 0.06 (9)
*p*CT	1.80 ± 0.03 (13)
*p*SCB	1.54 ± 0.04 (5)

The values of K_{IC} reported in this study are higher than those previously given by Sedighi et al [14] for thin (B = 4.7 mm) compact tension (1.28 MPa $m^{1/2}$) and SCB (1.30 MPa $m^{1/2}$) specimens. However, the fracture toughness values reported by Weerasooriya et al [15] for four-point bending experiments (1.42-1.68 MPa $m^{1/2}$) are in agreement with those obtained for the *p*SCB specimens. Interestingly, the K_{IC} results obtained by Ayatollahi and Saboori [16] for PMMA samples loaded under pure tensile conditions (1.7-1.8 MPa $m^{1/2}$) are in line with those of the *p*CT tests but not with those of *p*SCB tests. These results suggest that not only the loading conditions but also the specimen geometry have an impact in K_{IC} determination.

3.2. Photoelastic stress analysis (PSA)

Figure 5 shows some examples of the polariscope images resulting from the SCB and *p*CT tests. Isochromes are shown for the different loading levels. In the SCB test, the lack of control of crack propagation prevents stress assessment after P_{max}. It must be noted that in this study we focused on performing a qualitative analysis of the stress distribution from the images recorded, with the aim of identifying features having an influence on the results. However, a complete study of the stress field (i.e., the assessment of the direction and distribution of the principal stresses) is not reported.

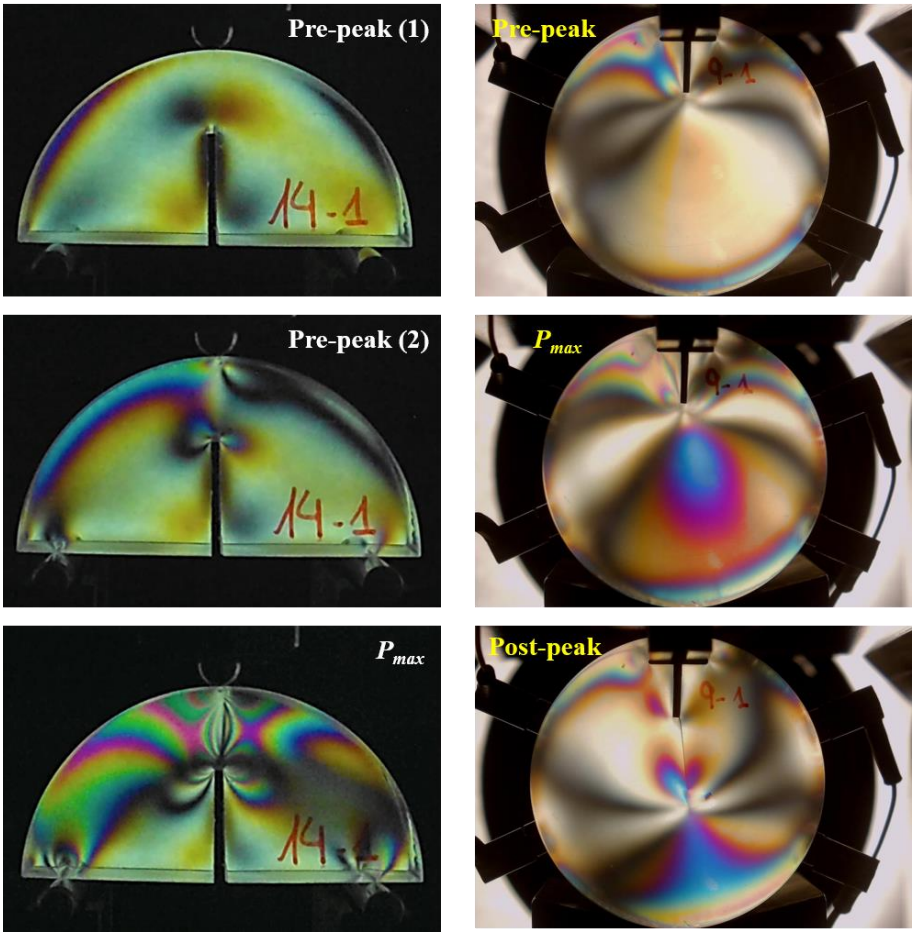

Figure 5. Time evolution of the stress field (from top to bottom) in SCB (left) and *p*CT (right) samples.

The fringe patterns observed in the pictures provide information about the distribution and concentrations of stresses. The colours of the isochromes appear in a sequence that is function of the stress level [17]. In the *p*CT test, we first observe fringes appearing mainly at the notch tip (the area where the highest stress should develop) which then extends towards the loading ends. The bottom part of the sample remains mostly unstressed. As the load increases, the first fringes move towards zones of lower stress and simultaneously, additional new fringes appear around the notch tip, indicating a growing stress concentration in this region. At P_{max}, the stress is located on the right side of the ligament plane, and we observe that the crack develops towards this area after peak load crossing. As the crack propagates, the stress is released at the notch tip and then mainly concentrates in the vicinity of the growing crack tip. In the case of the SCB test, high stress concentrations are observed not only at the notch tip, but also at the contact points with the rollers. At peak load, the high density of fringes observed at the top part of the sample would suggest a significant energy storage in this area [18], which then led to fast crack propagation with no post-peak control. The shape of the stress field at the notch tip (i.e., ellipses that become pointed at the tip) agrees with the prediction of the Linear Elastic Fracture Mechanics (LEFM) theory, less clearly for the *p*CT sample and better defined for the SCB specimen. Similar results were reported by Pitarresi et al [19] for epoxy samples loaded under three-point bending.

As previously mentioned, crack deviation from the ligament plane was observed in some experiments. In fact, the images resulting from the polariscope reveal that the stress field in the sample was not symmetrical, even for the SCB tests. The issue of fracture deviation has been previously observed in *p*CT and SCB tests performed with rocks [2,13] and was attributed to their likely heterogeneous and non-isotropic nature. However, crack deviation is also observed in this study for the homogeneous PMMA samples, which may be indicating that there might be additional features causing this behaviour. In this regard the asymmetric loading conditions, inherent to the *p*CT configuration and common in the SCB tests if the specimens are misaligned with respect to the top roller [12], could have a significant contribution. However, if that were the only cause for crack deviation, we would expect that crack development would always occur towards the same side of the specimens, at least in the *p*CT tests. Contrary, the deviation did not follow any discernible pattern, with specimens presenting cracks deviating towards either side. This was also previously observed by Muñoz-Ibáñez et al [2] for rock specimens. Therefore, there might be additional factors influencing fracture deviation. We conjecture that this could be related with imperfections in sample preparation (e.g., misalignment of the notch tip from the vertical plane or stress concentrations at the contact with loading ends) or the shape of the notch tip.

4. Conclusions

In this paper, a photoleastic stress analysis was carried to determine the stress field in mode I fracture toughness tests of PMMA samples. Tests were performed following three different testing methodologies: SCB, *p*CT and *p*SCB tests. The loading curves of the PMMA samples failed abruptly after the peak load, in agreement with the brittle nature of the material. However, despite this behaviour, the *p*CT and *p*SCB tests were able to provide control even in the post-peak region. The results of K_{IC} obtained in this study suggest a dependence on the loading conditions and on the sample geometry. The images from the polariscope revealed a high stress concentration at the notch tip (i.e., the point for crack initiation) and at the loading ends, especially in the case of the SCB tests. The stress field was asymmetric, and this behaviour would be caused not only for the asymmetric loading configuration but also for geometrical features such as imperfections in sample preparation. Our results revealed that these features can significantly influence the stress distribution in the sample and consequently play an important role in fracture propagation.

Acknowledgements

This work was funded by the MINECO/AEI/FEDER, UE project BIA2017- 87066-R.

References

[1] Zhang JJ 2019 Basic rock fracture mechanics *Applied Petroleum Geomechanics* (Gulf Professional Publishing) chapter 4 pp 133-61
[2] Muñoz-Ibáñez A, Delgado-Martín J, Costas M, Rabuñal-Dopico J, Alvarellos-Iglesias J and Canal-Vila J 2020 Mode I fracture toughness determination in rocks using a pseudo-compact tension (*p*CT) test approach. *Rock Mech Rock Eng* **53**(7) 3267-85
[3] Wu H., Golovin E., Shulkin Y, Chudnovsky A., Dudley JW and Wong GK 2008 Observations of hydraulic fracture initiation and propagation in a brittle polymer *The 42nd U.S. Rock Mechanics Symposium (USRMS), San Francisco, California*
[4] Phillips JW 1998 Experimental stress analysis *University of Illinois*
[5] Dally JW, Rilley WF 1991 *Experimental stress analysis* (New York: McGraw-Hill Book Co)
[6] Kuruppu MD, Obara Y, Ayatollahi MR, Chong KP and Funatsu T 2014 ISRM-suggested method for determining the mode I static fracture toughness using semi-circular bend specimen *Rock Mech Rock Eng* **47** 267–74
[7] Herbón-Penabad M, Muñoz-Ibáñez A and Delgado-Martín J (under review) Numerical and experimental analysis of pseudo-compact tension (*p*CT) testing configuration using two alternative sample geometries *EUROCK 2021, Torino, Italy*
[8] Laganà A, David M, Doutre M, de Groot S, van Keulen H, Madden O, Schilling M and van Bommel M. 2021 Reproducing reality. Recreating bonding defects observed in transparent poly(methyl methacrylate) museum objects and assessing defect formation *J Cult Herit (*Preprint*)*
[9] Samavedi S, Poindexter LK, Van Dyke M and Goldstein AS 2014 Synthetic biomaterials for regenerative Medicine Applications *Regenerative Medicine Applications in Organ Transplantation* (Academic Press) chapter 7 81-99
[10] Torabi AR, Saboori B, Keshavarz Mohammadian S, Ayatollahi MR 2018 Brittle failure of PMMA in the presence of blunt V-notches under combined tension-tear loading: Experiments and stress-based theories *Polym Test* **72** 94-109
[11] Visser HA, Caimmi F and Pavan A 2013 Characterising the fracture toughness of polymers at moderately high rates of loading with the use of instrumented tensile impact testing *Engineering Fracture Mechanics* **101** 67-79
[12] Hammer Ø 2011 *PAST PAleontological STatics Reference Manual* (Natural History Museum. University of Oslo)
[13] Muñoz-Ibáñez A, Delgado-Martín J and Juncosa-Rivera R 2021 Size effect and other effects on mode I fracture toughness using two testing methods *Int J Rock Mech Min Sci* **143C** 104785
[14] Sedighi I, Ayatollahi MR and Bahrami B 2020 A statistical approach on the support type effect on mode I fracture toughness determined using semi-circular bend (SCB) specimen *Eng Fract Mech* **226** 106891
[15] Weerasooriya T, Moy P, Casem D, Cheng M, Chen W 2006 Fracture toughness for PMMA as a function of loading rate.
[16] Ayatollahi MR and Saboori B 2015 A new fixture for fracture tests under mixed mode I/III loading *Eur J Mech A/Solids* **51** 67-76
[17] Vishay Precision Group 2011 *PhotoStress Instruments: Introduction to stress analysis by the PhotoStress method* (Technical Note TN-702-2)
[18] Ju Y, Ren Z, Mao L and Chiang FP 2018 Quantitative visualisation of the continuous whole-field stress evolution in complex pore structures using photoelastic testing and 3D printing methods. *Optics Express* **26** (5) 6182-201
[19] Pitarresi G, Toscano A, Scafidi M, Di Filippo M, Alessi S and Spadaro G 2014 Photoelastic stress analysis assisted evaluation of fracture toughness in hydrothermally aged epoxies *Frattura ed Integrità Strutturale* **30** 127-37